Dynamic study on Nanometer size square Permalloy (NiFe) antidot arrays; use as Monolithic Microwave localize band-pass filter

Bijoy K. Kuanr[*], Leszek M. Malkinski[**], Minghui Yu[**], Donald Scherer II[**], R. E. Camley[*] & Z. Celinski[*]

[*]Department of Physics, University of Colorado, Colorado Springs, CO 80918, USA
[**]Advanced Materials Research Institute, University of New Orleans, New Orleans, Louisiana 70148, USA

ABSTRACT

Nanometer sized Permalloy antidot arrays with different square hole sizes (1200 X 1200, 800 X 800, and 400 X 400 nm^2) have been fabricated by means of electron-beam lithography and lift-off techniques. We report here the dynamic properties of antidot arrays at GHz frequencies by using a flip-chip geometry and Network Analyzer based Ferromagnetic Resonance (NA-FMR) techniques. The dynamic excitations in the antidot arrays exhibit multiple resonance modes for the magnetic field applied in the plane of the array. Two distinct effective anisotropy field patterns split the uniform resonance into double resonance modes. The double resonance modes show uniaxial in-plane anisotropy and the easy axes are orthogonal. The magnitude of the induced effective anisotropy field decreases with the increase of square-hole size. The higher order resonance mode peaks move to low frequency with increase of the square-hole size at a constant applied field. We have demonstrated the possible application of antidot arrays as a magnetically tunable localized band-pass filter.

Keywords: Nano-holes, NA-FMR, spin dynamics, band-pass filter.

1 INTRODUCTION

The dynamic properties of magnetic nanostructures are drawing extensive attention due to their potential application for ultrahigh density data storage [1, 2]. It was proposed that a memory bit could be trapped between consecutive holes along the intrinsic hard axis of the antidot nanostructure [2]. One advantage of antidots over dots is that they can overcome the superparamagnetism limitation of isolated magnetic dots while preserving the properties of the magnetic film. This makes antidots a promising candidate for ultrahigh density data storage. One of the interesting dynamic phenomenona is the spin wave excitation, which arises as a result of quantization in small structures when the structure dimensions become comparable to the wavelength of the spin waves. Spin wave modes have been observed in magnetic dots and wires arrays with Brillouin light scattering (BLS) and ferromagnetic resonance (FMR) experiments. Though FMR is a powerful tool in investigating spin wave spectra very few FMR experiments have been conducted on such nano-magnets. Yu et al. [6, 7] studied the ferromagnetic resonances (FMR) in micron-sized square and rectangular Permalloy antidot arrays with circular hole size around 1.5 μm in diameter and separation from 3 to 7 μm. All the square and rectangular antidot arrays show double resonances with uniaxial in-plane anisotropy, which are the consequence of a dipolar field distribution producing two regions with different demagnetization field patterns [6]. In addition the main uniform mode, lateral spin waves were observed in antidot arrays which were attributed to lateral confinement from the vacant holes [7]. In this work, we have fabricated lithographically patterned antidot arrays with different nano-scale sizes of square holes on top of flat Si substrates. We performed a detailed Network Analyzer based FMR investigation in the frequency domain on the spin wave excitations in permalloy antidot arrays. A detailed study on the size dependences of the dynamic magnetic properties of these lithographically patterned nano-scale antidot arrays is presented.

2 EXPERIMENT

A Permalloy film with nominal composition of 81% Ni and 19% Fe and thickness of 100 nm was deposited [8] onto a resin by magnetron sputtering at the rate of 0.2nm/s at an Ar pressure of 3 mTorr. The thickness of the films was measured using a crystal growth monitor. Three square Permalloy antidot arrays were fabricated having a constant thickness of 100 nm using electron-beam lithography and lift-off techniques. First, a thin layer of polymethyl methacrylate (PMM) resist was spun onto Si(100) substrates, and then patterned with an LEO 1530 VP field emission scanning electron microscopy (FESEM) system operating at 30 kV. After development, a Permalloy film with thickness of 100 nm was deposited using a magnetron sputtering system with research S-gun and base pressure of $2X10^{-7}$ Torr. The argon pressure during deposition was 3.0 mTorr. The deposition rate was controlled by an INFICON IC 6000 quartz monitor and was kept at 0.2 nm/s. The Permalloy film was coated with a 5 nm Cu layer to prevent oxidation. Ultrasonic assisted lift-off in acetone was used to obtain the patterned antidot

NSTI-Nanotech 2008, www.nsti.org, ISBN 978-1-4200-8503-7 Vol. 1

arrrays. The whole antidot pattern consists of an array of 15 X 15 patches; the lateral size of each patterned patch is 100 X 100 μm^2. The spacing between each patch is around 10 μm, and the size of the whole pattern is 1.65 X 1.65 mm^2. The SEM images of the square arrays show well defined structures as seen in Fig. 1

In our earlier work [8], the static magnetic properties of these arrays were studied using a Quantum Design MPMS XL superconducting quantum interference device (SQUID) magnetometer at 300 K.

In the present work, a Cu-coplanar waveguide structure on a GaAs substrate was used as a transmission line to propagate an electromagnetic wave from a Network Analyzer. The width of the signal lines was 12 μm and the length of the device was 6 mm. The coplanar waveguides were designed for a 50 Ω characteristic impedance. The antidot array was flipped on top of the transmission line with the array length parallel to an external dc magnetic field. The frequency was swept from 0.05 to 40 GHz at zero or a fixed external magnetic field (H). The device characterization was done using a vector network analyzer along with a micro-probe station. Noise, delay due to uncompensated transmission lines connectors, its frequency dependence, and crosstalk which occurred in measurement data, have been taken into account by performing through-open-line (TOL) calibration using NIST Multical® software [14]. The exact resonance frequency (f_{res}) and frequency linewidth (Δf) [15] were obtained from Lorentzian fits to the experimental data.

3. RESULTS & DISCUSSION

The SEM images of the three antidot arrays with different square-hole sizes are shown in Fig. 1. Well defined square holes were achieved in the antidot arrays with hole widths of 1200, 800 and 400 nm. Decreasing the hole width to 400 nm causes the corner of the hole to be a little rounded. The spacing between the vacant holes is fixed at 400 nm for all the three antidot patterns.

Fig.2 shows the transmission response of the 800X800 nm^2 antidot structures. One sees two resonance modes of almost equal intensity. The first mode is at a lower frequency and the second is at a higher frequency in comparison to the single uniform resonance mode observed for a continuous Permalloy film of same thickness. For the antidot arrays, the uniform mode splits into two distinct resonance modes. In between these two resonance modes we observed a band-pass region (shown by a double arrow line in Fig.2), which can be tuned by an external magnetic field. It is also observed that the bandwidth of the pass-band increases with the increase in the square hole-size. This is because at a constant magnetic field (say 4 kOe); the higher resonance mode for all the three antidot arrays (S1-S3) occurs at the same frequency of 21 GHz,

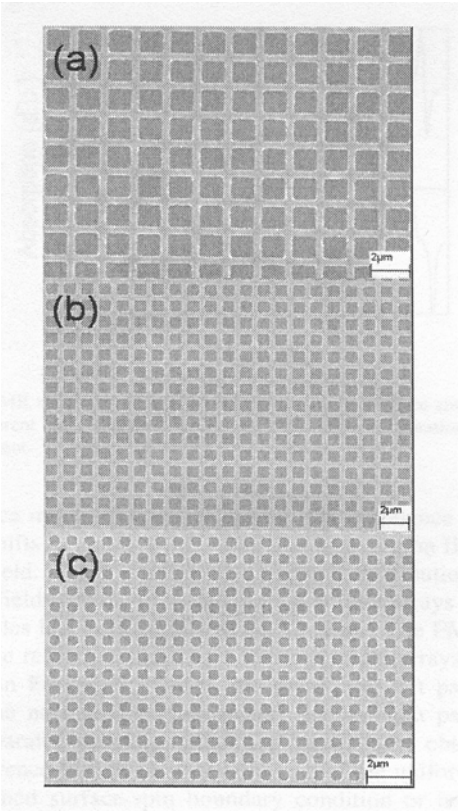

Fig. 1: SEM images of the antidot arrays with different square hole sizes: [(a) 1200 X 1200, (b) 800 X 800, and (c) 400 X 400 nm^2]. The separation between holes is 400 nm.

whereas, the lower resonance occurs at 16, 15 and 14 GHz for sample S1 to S3, respectively.

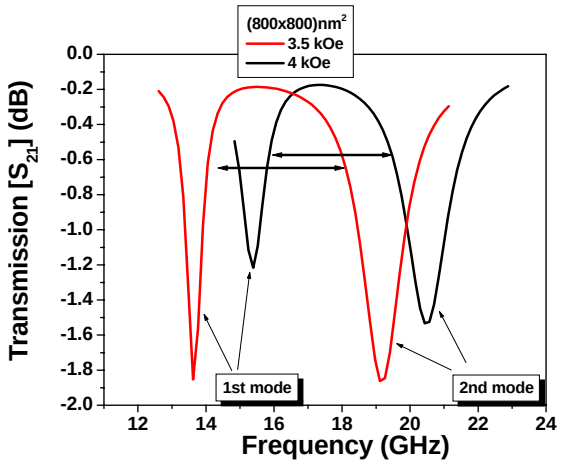

Fig. 2: The transmission response of the Permalloy antidot sample 800X800 nm^2 exhibiting double resonances at 3.5 and 4 kOe fields. The localized band-pass region is due to double notches.

In contrast, the continuous Py film resonance occurs at 18.5 GHz, i.e. in between the two modes of the antidot array. We also observed that the higher mode is broader than the lower mode. This may be due to multiple additional modes around that frequency, which are the outcome of the localized edge modes due to the sharp drop of the effective field near the hole edges.

Fig.3 shows the in-plane magnetic field dependence of both the modes for the 800 x 800 nm^2 (S2) antidot array along with the resonance frequency of the continuous Py film. When the magnetic field was along the plane, the sharp uniform precessional resonance mode was observed at lower frequency, and multiple resonance peaks also showed up at higher frequency. The multiple resonance peaks are associated with the excitation of quantized standing spin wave modes due to both the perpendicular and the lateral confinements [7, 9]. The double uniform resonance modes are originating from two regions experiencing different demagnetization field distributions.

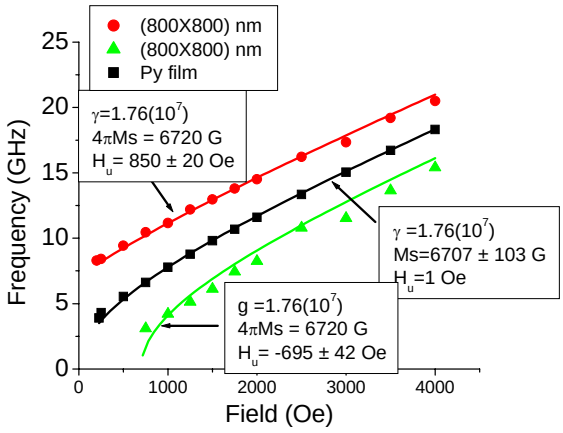

Fig. 3: Magnetic field dependence of double mode frequencies for sample S2 along with the frequency for a Py continuous film. The solid line is the theoretical fit to the FMR relation.

The inhomogeneous demagnetizing field has both static and dynamic components. When the field is applied along one side of a hole, the static magnetic poles are mainly distributed around the side perpendicular to the field. Therefore, the effective static dipole field has the opposite orientation of the external field in this case. In contrast, the long line of magnetic material parallel to the applied field will have some dynamic demagnetizing fields along its side edges. The distinct orientations of the effective fields in these two regions cause the split of the uniform mode. The theoretical fitting in Fig. 3 to these modes includes uniaxial in-plane anisotropy which is the consequence of effective fields with orthogonal orientation. In a microwave experiment, when the magnetic field is applied along the length of the hole, the spins precess in the uniform mode at FMR and they generate a demagnetizing field with its origin in the ‘‘magnetic charges’’ present on the surfaces. These local demagnetizing fields are responsible for the up-shifting of the second mode resonance frequency of the hole in comparison [5] to a continuous film. The absorption spectra of all the hole arrays show comparable line-shape.

One can use these ideas to obtain a simple, yet reasonable, estimate for the frequencies. We consider two fundamental elements: 1) a finite rectangular bar with its long axis oriented perpendicular to the applied field, and 2) an infinitely long bar of finite width with the long axis oriented along the external field. The Kittel formula [16]

$$f = \gamma\sqrt{(H + 4\pi(N_y - N_z)M_s)(H + 4\pi(N_x - N_z)M_S)}$$

gives the frequency as a function of the applied field H, the saturation magnetization M_s, and the demagnetizing factors N. For case (1) and using sample S2 above, the finite bar has a length of about 900 nm, a width of 400 nm and a thickness of 100 nm. This leads to demagnetizing factors $N_x = 0.712$, $N_y = 0.086$, and $N_z = 0.201$. For case (2) the length is infinite, and the width and thickness are the same as in case (1). This gives demagnetizing factors $N_x = .770$, $N_y = .230$, and $N_z = 0$. In Fig. 4 we present the resultant frequencies as a function of applied field.

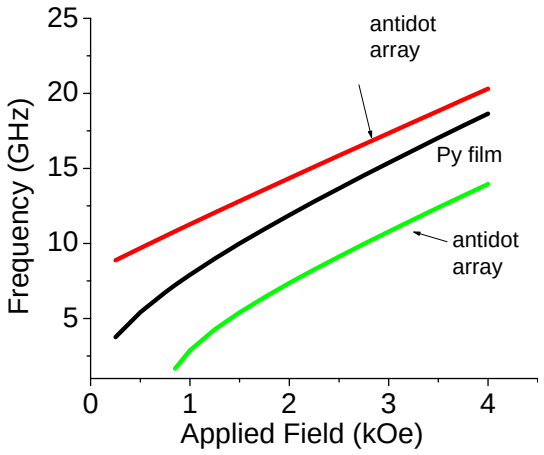

Fig.4: Simple estimate for the magnetic field dependence of double mode frequencies for sample S2 along with the frequency for a Py continuous film.

Considering the simplicity of the model, the result is surprisingly close to the experimental data of Fig. 3. We emphasize that the static magnetization patterns and dynamics can be much more complicated than the simple picture presented here as illustrated in Ref [17] Furthermore, it is not obvious whether one should use a finite or infinite length structure in case (1). Using the infinite length lowers the frequency of the lower mode by about 2 GHz. Nonetheless, Fig. 4 clearly shows the effective anisotropy is due to the structure of the antidot array.

NSTI-Nanotech 2008, www.nsti.org, ISBN 978-1-4200-8503-7 Vol. 1

Fig.5 shows the effective anisotropy field arising from the dipolar field distribution of the different antidot arrays as a function of the size of the antidot. The anisotropy field is observed to decrease with the increase of hole size. It is also observed that the frequency linewidth of the notches increases with the decrease in hole size.

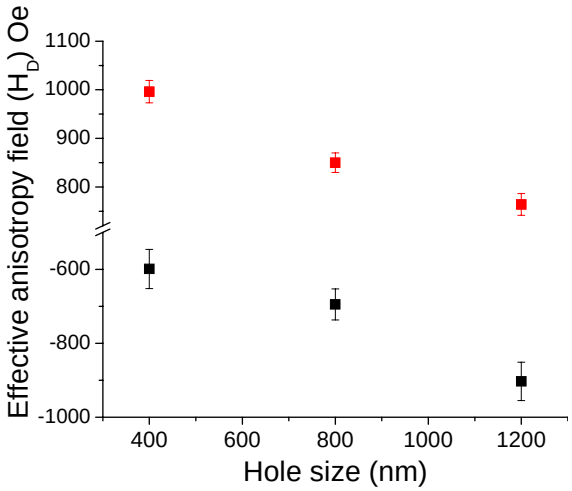

Fig. 5. Observed effective anisotropy field as a function of square antidot size.

4. CONCLUSION

Gyromagnetic resonance is observed using NA-FMR for Py antidot arrays. For an external field applied in the plane of the sample and along one side of the square, two resonances are observed. The frequencies of the resonances are controlled by the hole-size as well as by the applied magnetic field. We also observed that the frequency linewidths of the antidot arrays are dependent on the size of the hole. The two resonances can be modeled by introducing two distinct effective anisotropy fields. The magnitude of the induced anisotropy decreases with increase in the square hole size. The frequency linewidth of the higher order mode was observed to be larger than the lower one. The possible application of antidot arrays as a magnetically tunable local band-pass filter is shown.

The work at UCCS was supported by DOA Grant No. W911NF-04-1-0247

REFERENCES

[1]. L. Torres, L. Lopez-Diaz, and O. Alejos, J. Appl. Phys. **87**, 5645 (2000).
[2]. C. C. Wang, A. O. Adeyeye, and N. Singh, Nanotechnology **17**, 1629, (2006).
[3]. A. O. Adeyeye, J. A. C. Bland, and C. Daboo, Appl. Phys. Lett. **70**, 3164, (1997).
[4]. C. C. Wang, A. O. Adeyeye, N. Singh, Y. S. Huang, and Y. H. Wu, Phys. Rev. B **72**, 174426 (2005).
[5]. L. J. Heyderman *et al.*, Phys. Rev. B **73**, 214429 (2006).
[6]. C. T. Yu, M. J. Pechan, and G. J. Mankey, Appl. Phys. Lett. **83**, 3948, (2003).
[7]. C. T. Yu, M. J. Pechan, W. A. Burgei, and G. J. Mankey, J. Appl. Phys. **95**, 6648 (2004).
[8]. Minghui Yu, Leszek Malkinski, Leonard Spinu, Weilie Zhou, and Scott Whittenburg, J. App.Phy. **101**, 09F501, (2007).
[9]. M. Nisenoff and R. W. Terhune, J. Appl. Phys. **36**, 732 (1965).
[10]. P. E. Wigen, C. F. Kooi, and M. R. Shanabarger, J. Appl. Phys. **35**, 3302, (1964).
[11]. M. J. Pechan, C. T. Yu, R. L. Compton, J. P. Park, and P. A. Crowell, J. Appl. Phys. **97**, 10J903 (2005).
[12]. G. N. Kakazei, P. E. Wigen, K. Yu Guslienko, V. Novosad, A. N. Slavin, V. O. Golub, N. A. Lesnik, Y. Otani, Appl. Phys. Letter, v.85, p. 443 (2004)
[13]. G. Gubbiotti, Phys. Rev. B, v.72, p.224413-1 (2005)
[14]. R. B. Marks, IEEE Trans. Microwave Theory Tech., vol. 39, p. 1205, (1991).
[15]. Bijoy K. Kuanr, R. E. Camley and Z. Celinski, Applied Physics Letters, **87**, 012502 (2005).
[16] C. Kittel, Phys Rev., **73**, 155 (1948).
[17] I. Guedes, M. Grimsditch, V. Metlushko, P. Vavassori, R. Camley, B. Ilic, P. Neuzil, and R. Kumar, Phys. Rev. B **67** 024428 (2003)